3

Bio-Chemical Sensors based on Molecularly Imprinted Polymers; Soft Lithography, Microfabrication and Microfluidic Synthesis

Kyung M. Choi

Department of Chemistry, University of California at Irvine, Irvine, CA 92697

Outline

Introduction

Nanotechnology has brought us numerous innovations to improve the quality of our lives by opening new areas that have never been explored. Theory of quantum dots has been significantly investigated to emerge novel advantages derived from the small size. [1-2] There are many challenges for chemists to play an important role in this area by employing chemical strategies since nanotechnology is a part of the chemical domain, which builds up new materials at the nano-scale.

Recent advances in nanotechnology include organic transistor/flexible electronics [3-8], soft lithography [9-16], micro contact printing [17], flexible bio-devices [18-19], and microfluidic synthesis. [20-30]

This technology also brings us a new era in sensor technology. [31-33] For sensor applications, unconventional approaches in the development of sensing materials and fabrication techniques have been widely investigated to achieve high performances such as prompt detection, high sensitivity, low cost, greater fidelity, and high reliability and thereby offer promises for innovations in sensor technology.

Many types of sensing materials have been discovered and then widely used to fabricate a variety of sensors or detection devices. For example, a) physical sensors based on flow, stress, strain, position, particles, or force, b) chemical sensors based on chemicals/molecules and concentration, c) biosensors based on bio-active elements.

Recently, novel nanomaterials have taken a considerable attention for sensing applications. [31, 32] For example, Huang X. J. et el published a comprehensive review of chemical sensors based on nanostructured materials. [31] They investigated on several sensing materials at the nano-scale; a) nanotubes, b) nanorods, c) nanobelts, and d) nanowires to direct and thus to lead this area. Guo X. also published a review on biosensors based on single-wall carbon nanotubes. [32] This review addresses the molecular structures, interacting dynamics, and molecular functions in the field of single molecule biosensors and practical applications, such as the device reproducibility, system integration, and theoretical simulation.

Microfabrication technique also has been studies to build up small-sized sensors, which produce a set of advantages including lower power consumption, wearable design, integrated circuit feature, and light weight. [33] This technique can be used to fabricate a range of different microsensor platforms on a small chip by using small amounts of materials/chemicals in fashionable patterns.

In this chapter, we will introduce both of organic sensing materials and microfabrication techniques to achieve small-sized chemical sensors with high performances.

Chemists have been seeking for unusual routes to synthesize novel sensing materials; considerable researches on the development of new sensing materials have been carried out. In sensor technology, enhancement of the sensitivity is a key contributor to the improvement of device performances. However, conventional synthetic approaches on sensing materials often limit to satisfy our diverse demands in detection technology.

Understanding both of chemistry and fabrication techniques are critical to design a new version of sensors, especially active sensing devices with high selectivity and sensitivity. The physicochemical properties of conventional sensing materials are usually not sufficient enough to establish an unambiguous sensor classification; advanced sensors that have more than one property are desperately required. The size and scale of sensors are also important due to our growing demand in nanotechnology.

Due to our stringent needs for more compact and multifunctional sensors with multiple properties, an incentive exploration in the synthesis of novel sensing materials and fabrication techniques currently lead this area.

Many advances, especially in device fabrications on a chip, have been achieved by emerging diverse technologies from physicists, chemists, engineers, biologists, and material scientists. There are many challenges for chemists to contribute to this area. Due to recent advances in nanotechnology, we employ nanotechnology for sensor applications to meet our diverse needs in detection technology.

Unconventional approaches have been examined to fabricate more compact devices in nanotechnology; for example, soft lithography, microfabrication, microfluidic synthesis, and flexible electronics are discovered and then widely investigated to expand the scope of this area. [3-30]

For example, soft lithography has taken a significant attention; because, it offers an easy and low-cost patterning transfer in the integration of nano- or micro-devices by fabricating electronic circuits on flexible substrates. [9-16] Soft lithography is an alternative to a conventional UV photolithography to replicate and then transfer small patterns from the original masters to substrates. Recently, intensive efforts on the development of wearable electronics or bendable displays are focused on research projects; non-silicon electronic technology, which is soft lithography can be used for this type of applications.

Soft lithography uses soft elements such as silicon rubbers as a Mold or a Stamp; the stamp will transfer small patterns from the original masters to a variety of substrates. The stamp can be also used to carry out the contact-printing technique. [17] A silicon rubber, poly(dimethyl)siloxane (PDMS), has been widely used in soft lithography as a mold (stamp) to directly replicate and thus to integrate small patterns on flexible substrates.

However, soft lithography often limits on pattern transferring tasks due to its insufficient mechanical strength of commercial PDMS silicon rubbers; because, commercial PDMS materials have been developed for other applications. To improve the performance of soft lithography, we employed a chemical strategy, which designed a new molecular structure of silicon rubber to create our desired properties for our soft lithographic purposes.

Usually, the resolution of soft lithography significantly relies on stamping elements. However, a commercially available silicon elastomer, PDMS, has shown mechanical failures; for example, during the pattern transfer, commercial PDMS stamps often result in collapse and mergence due to their low mechanical property, especially in the nano-scale regime.

The limitations have motivated us to develop a new version of silicon elastomers. A new PDMS prepolymer was molecularly designed to create a set of our requirements for soft lithographic performances such as high physical stiffness, high elastomeric property, low linear polymerization shrinkage, photocurability, and freedom from stress. The resulting PDMS mold has shown an enhanced performance in soft lithographic capability. [14,15] Furthermore, the new PDMS prepolymer is based on a photocurable prepolymer, which is photopatternable; therefore, it can be photopatterned on a chip with fashionable features.

In this chapter, microfluidic technology is also presented to synthesize novel sensing materials/particles at a low cost. [20-30] One of pioneers in this technology is Quake; his research group has published a leading technology, a large integration of microfluidic reactor. [20]

This technology employs microfluidic reactors to produce materials/particles with a continuous production capability at the nano- or micro-scale. Various chemical reagents and carrier fluids have been selected and then injected into microfluidic reactors, which are specially designed their channel patters for our diverse applications. Subsequently, micro-droplets are generated at the T-junction where multiple reagents are fused. [20-30]

Furthermore, microfluidic reactors enable to produce materials with specific advantages, which can't be available from conventional synthesis. For example, the use of microfluidic reactors often results in high product yields by mixing of multiple reagents at the micro-scale and quenching sequences for greater reaction selectivity in the reactors.

Chemical homogeneity can also be beneficial; because, the synthetic condition at the micro-scale is liable to influence the nature of materials and to eliminate local variations. Such a mixing at the micro-scale in the microreactor can be mediated and thus the entire reaction volume can be held at uniform condition.

In addition, microfluidic reactors can be coupled to next processing steps and transported directly for the integration into devices. Desired materials with narrow molecular weight distributions are produced in the microfluidic reactors and are available for processing, such as further mixing, deposition, or coating on surfaces. It is also a low cost process, which produces desired materials by a continuous production and using small amounts of multiple reagents at a highly controlled condition. A number of studies have been published to demonstrate specific advantages of microfluidic technology which can't be achieved from conventional synthesis. [20-30]

For example, Beers' group has published a microfluidic synthesis of photocurable polymers using a microfluidic reactor. [22] They reported the use of microfluidic synthesis to create a new physicochemical environment for continuous, controlled radical polymerization. They demonstrated a photopolymerization in the microfluidic reactor by taking an advantage of its low oxygen permeability and good pressure stability.

Haeberlea et. al. also published a paper, the synthesis of polymeric particles in microfluidic reactors for continuous productions. [27] Their method includes (a) the generation of highly monodisperse monomer droplets in a microfluidic flow-focusing device and (b) in-situ solidification of these droplets by means of photopolymerization.

They also demonstrated the effect of monomer properties on the emulsification process; the effect of the polymerization rate on the production of high-quality particles, the role of the material of the microfluidic device in droplet formation, and the synthesis of particles with different shapes and compositions. They also demonstrate the production of highly ordered arrays of polymer particles achieved by photopolymerization of the dynamic lattices of monomer droplets in microfluidic channels.

In this chapter, we introduce a novel sensing material, "Molecularly Imprinted Polymers (MIP)." [34-46] MIP's system has been widely used to develop sensors or chemical detection devices. MIP's system has "high affinities receptors or binding sites" to detect specific target molecules for molecular detections. Synthesis of "high affinity receptors or binding sites" is a key contributor to achieving high performance sensors.

The molecular recognition sites in MIP's system can be provided by "Molecular Imprinting Technique," which is a general protocol for the creation of "synthetic receptors or binding sites" with specific molecular recognitions in cross-linked networks. Target molecule is called a template, which is used to create synthetic receptors or binding sites. Molecular recognition takes place by a rebinding process to the receptors.

However, a practical application of MIP's sensors has limited due to the lack of materials' properties or integration-techniques or low sensitivity. To improve the performance of MIP's based sensors, we demonstrate new approaches in this chapter. To fabricate small-scale sensors, we present a microfabrication of MIP's photocured patterns. To increase the sensitivity of MIP's based sensors, we also introduce a microfluidic synthesis of MIP's particles by using a microfluidic reactor, which was specifically designed for the synthesis of MIP's small particles.

Material Property

Molecularly Imprinted Polymer (MIP)

"Molecularly imprinted polymer (MIP)" has been considered as a promising sensing material due to synthetic receptors or binding sites, which have specific molecular recognition. [34-46]

MIP's system is a highly cross-linked macro-porous thermoset with high internal surface areas and recognition sites. MIP's system can be produced by "Molecular Imprinting Technique," which is a chemical process for the synthesis of functional groups that contain recognition sites. Molecular recognition takes place by a rebinding process using a porogen.

Figure 3.1 illustrates a molecular imprinting process to synthesize recognition sites. It is a schematic diagram of the formation of synthetic receptors by a copolymerization of functional monomers and cross-linking monomers in the presence of imprinting molecules (template, denoted as 'T' in Figure 3.1).

As shown in Figure 3.1, the imprinting process involves an interaction between the functional monomer and the template molecule, target molecule. The functional monomer contains a

chemical functionality that reacts with the template molecule by a chemical interaction between the functional monomer and the template. The interaction results in a self-assembly system.

Subsequently, the self-assembly element will be copolymerized with excess cross-linking monomers to produce an imprinted system, which is a highly cross-linked (> 50 %) macroporous thermoset.

After the copolymerization with the cross-linking monomers, the template can be extracted and then create "receptors or biding sites" in the cross-linked polymeric network. "Molecular recognition" will take place by a rebinding process of the template to the imprinted sites.

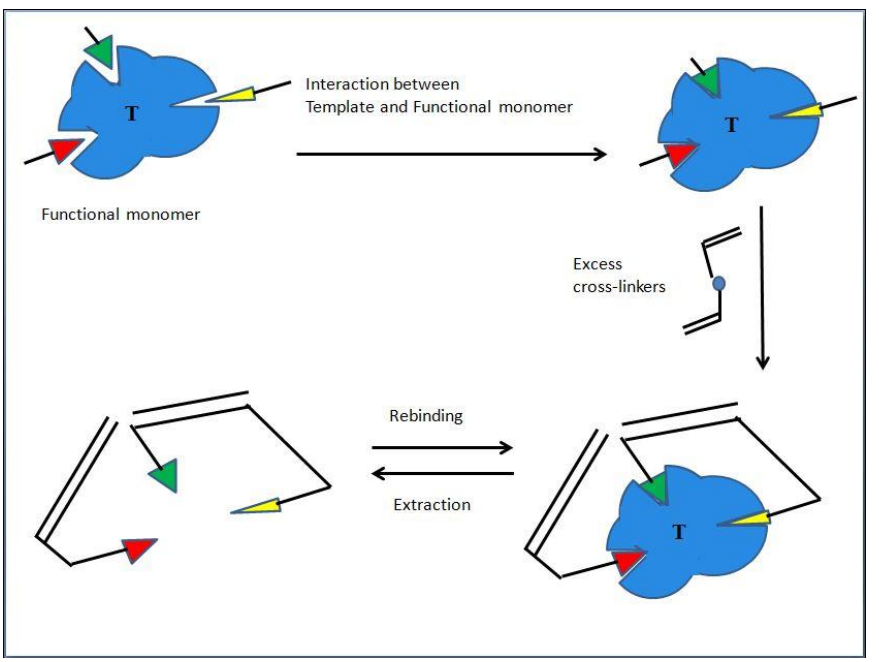

FIGURE 3.1
Molecular imprinting technique to synthesize receptor or binding sites. 'T' stands for a template molecule

As shown in Figure 3.1, this technique uses a small single molecule as a "Molecular Mold." For this reason, the molecular imprinting technique is a kind of molecular level lithography; the molecular mold is called "template molecule."

MIP's system has been investigated for a wide variety of applications, especially as a sensing material due to its targeting molecular recognition. The applications include chromatographic stationary phases, solid phase extraction materials, selective absorptions, catalysts, and bio-chemical sensors. The majority of MIPs' system is based on organic polymers that are prepared by radical polymerizations. Vinyl and methyl acrylic monomers are also used as functional monomers for the imprinting process. Various solvents can be used as porogens to extract templates and thus to create 'receptors or binding sites' in the imprinted networks.

Noncovalent or Covalent Imprinting Technique

In the molecular imprinting technique, a template or a target molecule can be imprinted by either a non-covalent [36] or a covalent [37, 39, 41, 43, 44] method.

The non-covalent imprinting process employs a self-assembly strategy in which a functional monomer and a template are pre-assemble by a non-covalent bonding such as a hydrogen bonding, electrostatic and/or van der Waal's forces.

The self-assembly system is then copolymerized with a cross-linking agent to provide a polymeric network. Subsequently, the template can be removed by an extraction with a solvent system leaving behind the complementary binding sites. In non-covalent imprinting technique, the template and the receptor are non-covalently linked each other by week chemical bonds. For this reason, the template can be easily washed away and then rebound to the imprinted receptors to take place "molecular recognitions."

In contrast, the covalent method involves a synthesis of a template, which is covalently linked to a functional monomer through a relatively labile chemical bond. Subsequently, a copolymerization with a crosslinking monomer results in a networking polymer. In this case, the template can be extracted by a chemical cleavage, leaving behind highly ordered binding sites.

High Affinity Distribution

Molecular imprinting technique has been used to produce novel materials for sensors or environmental catalysts. Chemical recognitions and catalytic sites can be created in cross-linked polymers with molecular recognition groups, which will react to templates.

For biosensor applications, specific recognition sites of complex molecules and biological entities have been created to develop bio-sensors, diagonostic medical detections, and drug delivery devices; molecular imprinting technique has been employed to create "polymeric receptors," for example, DNA and RNA bases have been also investigated. [18, 35-45]

However, a practical application of MIP's system limits due to low sensitivity.

Since detection is elicited by changes in the physicochemical property of the molecular interfaces, the development of "high affinity binding sites" on molecules is significantly required to achieve a high affinity and high sensitivity.

To enhance the sensitivity of MIP's based sensors, a challenge to synthesize 'Monoclonal' MIP's particles was demonstrated in this study by employing microfluidic technology; the "monoclonal" means a system that has high affinity binding sites only.

To achieve a high affinity in MIPs' system, an intensive research on the synthesis of small-sized MIPs' particles was carried out; because, the particle sizes of MIP are directly related to their affinity capability of specific molecular recognition.

According to a previous study, the distribution of molecular recognition affinities significantly relies on the recognition capability; nonspecific binding sites would result in false positives or high background signals in chemical detections. [42] They presented a connection between particle sizes and number of binding sites per particle; *their affinity distribution indicates that "high affinity binding sites" could be obtained when the number of binding sites per particle decreased*. [42]
For this reason, the production of 'monoclonal' particles relies on the synthesis of mono disperse smaller particles.

In other words, that nano-sized particles will have more chance to produce single site entities; for example, reduction in the size to the nano-scale would have more chance to produce a particle with more high affinity sites per particle. The number of sites per particle, the mass of the particle, is also reduced as the size of particle is reduced.

To obtain high affinity sites, particles with low or no affinity need to be removed by an affinity separation to select mono disperse particles only. For example, when MIP's particles at >1μm possess a mixing of low and high affinity sites, those low affinity sites would decrease recognition sensitivity in MIP's system.

For this reason, the production of nano- or micro-sized MIPs' particles is a key object to the synthesis of 'monoclonal MIP particles,' which would have high affinity binding sites only. Thus, our effort focused on the production of smaller MIP's particles to enhance the sensitivity of sensors.

Challenge on the synthesis of 'monoclonal' MIPs' particles, which has only high affinity sites, is desperately needed to achieve a high selectivity and sensitivity since a practical application of MIP limits due to the low affinity sites.

In short, the production of 'monoclonal' MIPs' particles relies on the synthesis of mono disperse imprinted MIP's particles at the nano-scale; because nanoparticles would contain a distribution of affinities but are of a size that will permit separation based upon their affinity, such as an affinity separation of proteins and antibodies. [46]

Sample Preparation [26, 39]

MIP's monomer mixtures can be prepared depend upon specific target molecules, templates. Figure 3.2 illustrates an example of the preparation of a MIP's monomer mixture that contains "9-ethyladinene (9-EA)" as a target molecule.

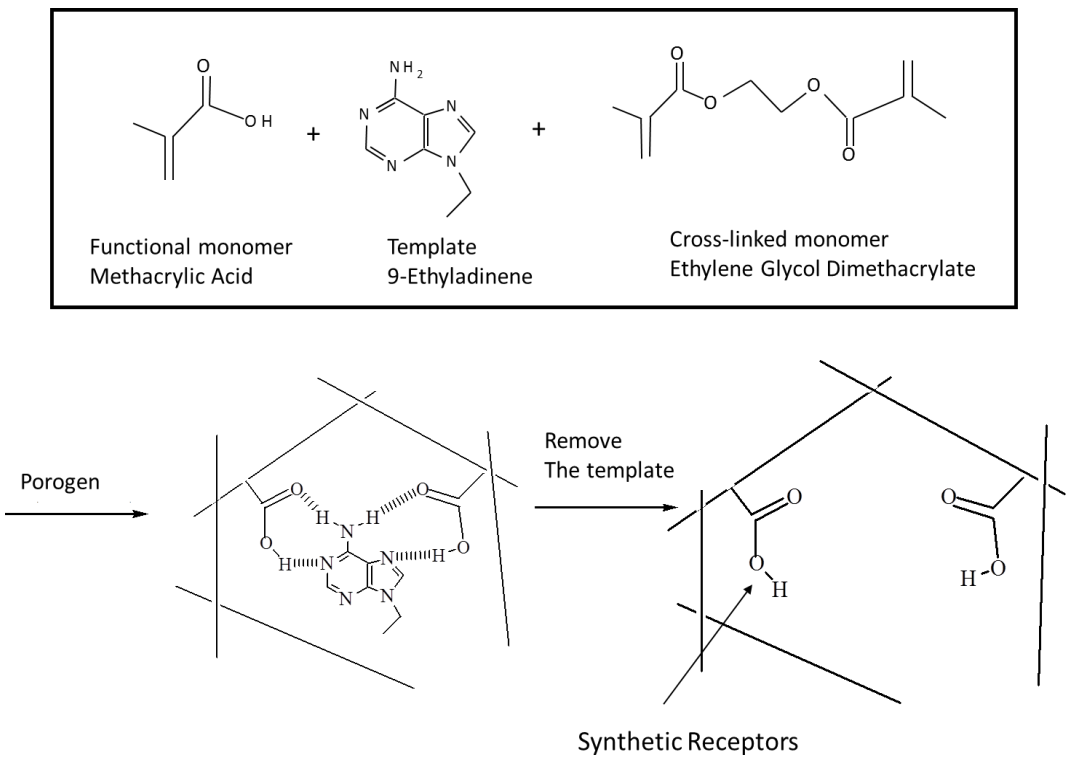

FIGURE 3.2
Preparation of a MIP's mixture based on a template, 9-ethyladinene; the arrow is a receptor or a binding site, which has a recognition function [26, 39]

Soft Lithography

Soft lithography has been intensively investigated to improve patterning transfers from the original master to the substrate, especially for flexible electronics. [9-16] Soft lithography is a cheap lithography, which is an alternative to conventional photolithography. Soft lithography uses elastomeric elements, silicon rubbers, as a stamp or a mold or a conformable photomask for patterning transfer tasks.

Figure 3.3 shows soft lithographic processes, a) Making the mold (or stamp) from the original master, b) Stamping process using the mold, and c) Microcontacting process.

a) Making the mold (or stamp) process produces a thermally cured PDMS mold (stamp) with a surface relief feature from the original master. b) The PDMS mold (stamp) can be used for stamping the features from the masters onto a variety of substrates; this is a low cost process of patterning transfers at room temperature. c) The PDMS mold (stamp) also can be used for the micro-contact printing, especially on the gold layer by a self-assembly process. [17]

However, the physical property of commercial silicon elastomers limits for our lithographic purposes, especially in the nanometer regime; because, silicon rubber-based PDMS stamps were developed for other applications and thus are susceptible to fracture if the physical toughness is insufficient for our lithographic purposes; especially, tall and narrow features of surface relief are unstable to mechanical collapse when the modulus of stamps is too low.

Past works in soft lithography have relied primarily on stamping materials made with commercially available silicone elastomers that were not designed for our soft lithographic purposes. The desired physical properties of stamping materials include (1) the ability to photocure (to avoid thermally induced stresses and shrinkage and to enable photopatterning capability), (2) high modulus (20 MPa represents a relevant range), with the ability to tune this property, (3) high physical toughness (> 0.1 MPa), (4) low polymerization induced shrinkage (< 1 %), and (5) low thermal expansion coefficient (< 300 ppm). [14, 15]

The limitations of commercial PDMS stamps motivated us to develop a new version of PDMS elements, which was molecularly designed to meet the set of our multiple requirements in patterning transfers. This chapter introduces a novel chemical strategy to create a new version of PDMS stamps, which was specifically designed for our soft lithographic purposes at the nano-scale.

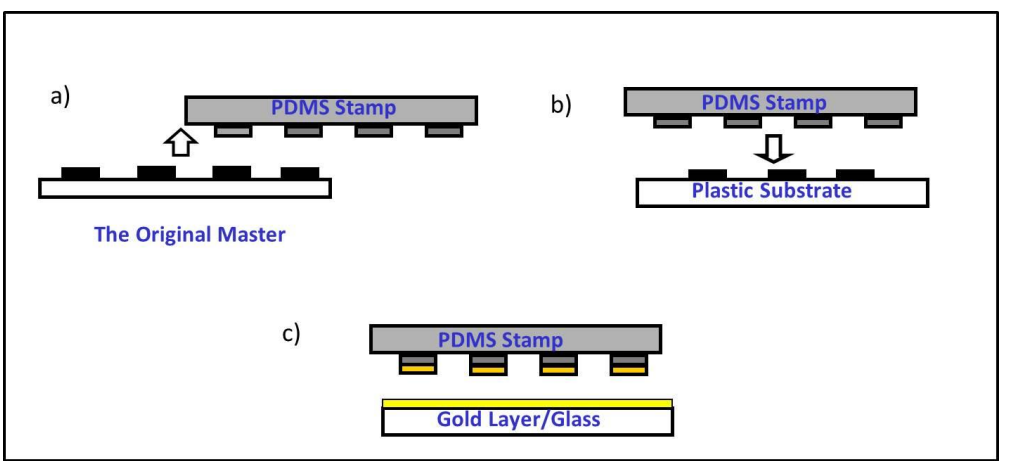

Figure 3.3
Soft lithography; a) Making the stamp (or mold), b) Stamping process, and c) Microcontacting process

Experimental details

a. Making a Mold [14, 15]

An original master with desired features was prepared by UV photolithography using a quartz mask. The surface of the silicon wafer-based original master was fluorinated using tridecafluoro-1,1,2,2-tetrahydrooctyl-1-trichlorosilane (Gelest, SIT8174). The fluorinated master was then placed in a plastic container. A mixture of PDMS prepolymer was poured onto the fluorinated master. For the case of thermocured system, the sample container was placed in a vacuum desiccator to

remove bubbles. The PDMS mixture was thermally cured in an oven at 60 °C for 12 h. In the case of photocurable system, the PDMS mixture was poured onto the master and then irradiated with a UV lamp (UVP Blak-Ray, B100AP; 365 nm long wavelength) under a nitrogen for 10 min. After the curing processes, the thermocured or photocured stamps (molds) were carefully peeled off from the masters and then cut out using a razor blade.

b. Stamping Process [14, 15]

An optical adhesive (Norland, NOA 72) was used for the stamping process. A cured PDMS stamp was cut out from the master. A few drops of the optical adhesive liquid were applied on a cleaned glass slide. A PDMS stamp was then carefully placed on the top of the optical adhesive layer. Bubbles between the adhesive layer and the stamp were removed. Subsequently, UV irradiation followed to cure the adhesive layer through the PDMS photomask for 1 h. After the photocuring process, the PDMS stamp was carefully peeled off. Surface relief features were generated on the cured adhesive layer. The cured adhesive was then treated with a "gold sputter" for scanning electron microscopy (SEM) analysis.

c. Microcontact Printing Process [17]

For the microcontact printing process, we used the PDMS stamp that was "inked" with a solution of alkanethiol in ethanol to build up self-assembled mono-layers on the gold surface. Sylgard 184 stamp has been widely used for the microcontact printing process due to its good surface adhesion.

In this process, a cleaned glass slide was prepared for a gold deposition process. A 10 Å thickness of titanium layer was first deposited on the glass as an adhesion promoter at a deposition rate of 3 Å/s, followed by 200 Å of gold layer on the top of the titanium at a deposition rate of 10 Å/s using an electron-beam evaporator.

The PDMS stamp was brought into a close contact with the gold layer after inking the stamp with 3 mM of 1-hexadecanethiol (Aldrich, H763-7) in ethanol. After the close contact for approximately 15 s, the glass was soaked in a gold etching solution, a ferricyanide enchant, for about 7 min; a fresh gold etching solution was provided each time from an aqueous solution containing KOH (16.8 g), potassium ferricyanide (III) (1.09 g), potassium ferrocyanide (II) trihydrate (0.13 g), and sodium thiosulfate (7.4 g) in 300 mL of water. After this etching process, the glass was washed with water, followed by complete drying using a nitrogen gun.

New Stamps

The most widely used silicon elastomers for soft lithography is "Sylgard 184" (Dow Corning), which consists of a silicone "T-resin" cross-linker by a mixture of vinyl-terminated poly(dimethyl)siloxane and trimethylsiloxyterminated poly(methylhydro-siloxane) prepolymers. The resulting stamp (denoted as "184-PDMS") has a highly cross-linked three-dimensional structure after thermal curing process; 184 PDMS stamp offers a high elongation at break but a relatively low modulus that can lead to structural problems in the patterning transfer process, especially for features at the nanoscale. [14, 15]

An IBM research group developed PDMS elements with relatively high compression moduli using commercially available silicon rubber elastomers [11, 13]; the resulting stamp (denoted as "h-PDMS") was prepared from a couple of commercially available materials, trimethylsiloxyterminated vinylmethylsiloxane-dimethylsiloxane (VDT-731; Gelest) and methylhydrosiloxane-dimethylsiloxane (HMS-301; Gelest) copolymers.

The h-PDMS stamp has cross-linkers that have relatively short lengths as compared to those in the 184-PDMS system. As a result, the h-PDMS stamp shows a relatively high modulus, but its elongation at break is much lower than that of 184-PDMS. Composite bilayer patterning elements that use a thin layer of the h-PDMS with a thick backing of 184-PDMS effectively combine some of the attractive features of these two PDMS silicon rubbers for certain applications. [14, 15]

To reduce a shrinkage from the thermal curing process, we considered a commercial photocurable PDMS system (RMS-033; Gelest). The chemical structure is based on a (methacryloxypropyl)methylsiloxane-dimethylsiloxane copolymer. However, in our experiments, the resulting photocured PDMS (denoted as "s-PDMS") has shown an insufficient modulus that was not usable for soft lithographic purposes. [14, 15]

To improve the mechanical property of commercially available PDMS materials, we designed a novel chemical structure of PDMS prepolymers as shown in Figure 3.4; the new structure was specifically designed for our soft lithographic task to create desired properties.

The new molecular structure also provides a flexibility for adjusting the material properties to match our demands on patterning transfer task. In Figure 3.4, the bold lines correspond to the designed cross-linkers, "urethane methacrylate groups".

The overall structure of new PDMS is shown in Figure 3.4.

In our chemical strategy, urethane functionality was inserted into the cross-linkers to improve the physical toughness; urethane groups serve as the rigid and flexible cross-linkers. Methacrylate group was also inserted into the cross-linking networks to create a photocurable capability for reducing the thermal shrinkages. The resulting PDMS stamp is defined as "hù-PDMS stamp."

The hù-PDMS prepolymer is based on a long, linear PDMS chain that is already prepolymerized but which remain in a viscous liquid phase. The prepolymerized system would minimize polymerization shrinkages associated with photocuring processes.

We begin by outlining the chemistry and mechanical properties of PDMS systems and their relationships to previously explored elements. [14, 15] We demonstrated its use in representative soft lithography that highlights some of its attractive features.

In DMA (Dynamic Mechanical Analyzer) experiments, the length and stiffness of hù-PDMS stamps lie between those commercial PDMS stamps that are used in the 184-PDMS and h-PDMS systems. The new PDMS prepolymer shows many improved mechanical properties that are attractive for our soft lithographic purposes, especially for nanopatterning applications.

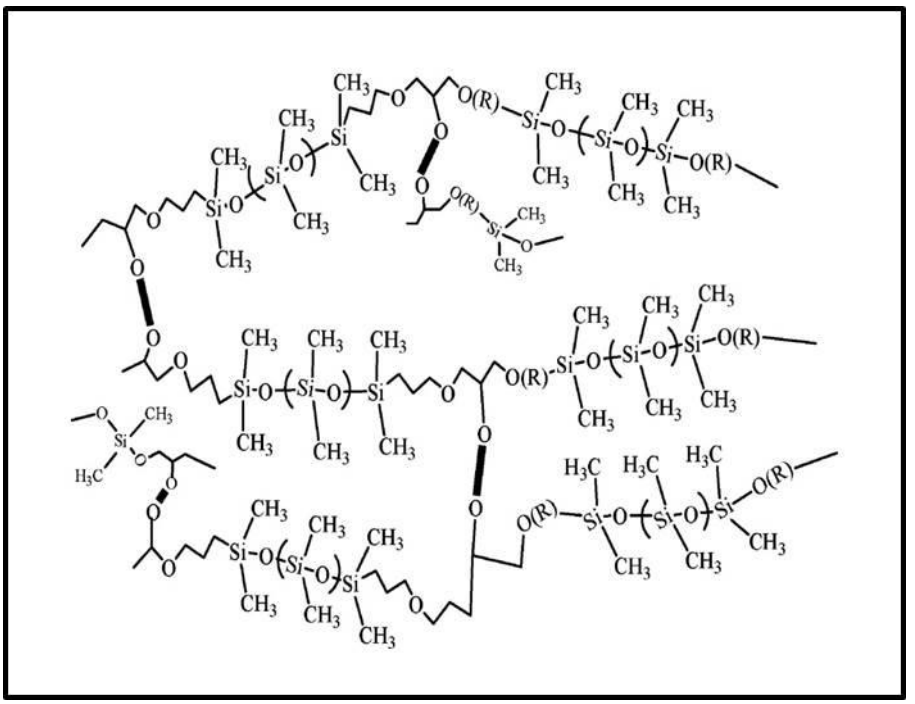

FIGURE 3.4
Chemical structure of hù-PDMS prepolymer; the bold lines correspond to urethane-based cross-linkers

Mechanical property

Commercial PDMS prepolymers have been widely used in soft lithography; however, those commercial silicon rubbers limit in lithographic tasks due to the lack of mechanical strengths. For example, h-PDMS stamp developed by an IBM group [11] tended to fail due to fracture of the relief features during fabrication of the elements or during their use, particularly in molding applications. We believe that the relatively low physical toughness of h-PDMS makes relief features with these geometries susceptible to fracture.

To achieve a high fidelity in soft lithography, hù-PDMS stamp has been developed and then examined. [14, 15]

Mechanical strength measurements of PDMS stamps were carried out by using a DMA analyzer (Perkin-Elmer, DMA-7E) to determine compression modulus, tensile modulus, and elongation at break.

The static compressive, dynamic compressive, static tensile, and dynamic tensile moduli of h-PDMS, hù-PDMS, s-PDMS, and 184-PDMS stamps were measured at room temperature in air. A 184-PDMS stamp was used as a standard material. For compressive modulus tests, those PDMS prepolymers were cured into a disk molder of ~2 mm in thickness and 3 mm in diameter to prepare disk-type samples.

To establish the relative hardness of these silicon elastomers, the resistance to indentation by a 3 mm diameter cylindrical, stainless steel probe mounted in DMA was determined as a function of load. These data for indentation versus force were then recalculated in terms of stress/strain to compute compressive modulus from the slopes in linear portion of the static compressive stress/strain curves. In static tensile measurements, the static force on each sample was initially 5 mN and the load was ramped to 8000 mN or until rupture with a rate of 500 mN/min. In this test, the dimension of each PDMS sample was 0.3 × 3.5 × 5 mm (thickness × width × length).

Static tensile moduli of four PDMS systems were then calculated from the slope of the static tensile stress/strain curves in a linear region of the curve. Elongation at break was also obtained from the static tensile stress/strain plots when rupture occurred. Physical toughness was computed from the area under the static tensile stress/strain curves. During the static tensile test, we observed that the thin PDMS films were difficult to handle due to slipping in the DMA's steel clamps at high forces during elongation.

We also observed some rupturing at the edges of those thin PDMS films. For this reason, we only accepted elongations at break if the rupture has occurred at the center of PDMS films. In this way, one can assume the clamp hardware has not influenced the breaking of a film. Dynamic compressive moduli of the four stamps were also provided by oscillating DMA measurements at 1 Hz in air using stainless steel hardware with 3 and 8 mm in diameters of the upper and the lower plates, respectively, to double-check their static values.

It was carried out at 3% constant strain to eliminate surface effects on the dynamic moduli values. We also carried out the dynamic tensile analysis at a small, fixed strain of 0.4 % and 1 Hz to double-check the static tensile determinations since one concern is sample slippage inside the DMA's clamping system during the static tensile tests.

Figure 3.5 (left) and (right) shows the static compressive moduli and the static tensile moduli of four PDMS stamps, respectively.

In the mechanical tests, the stress and strain curve of hù-PDMS stamp lies between 184-PDMS and h-PDMS curves; the data also show that s-PDMS has a modulus that is much too low for most applications in soft lithography.

In Figure 3.5, the physical toughness (as evaluated from the area under the stress/strain curve) of hù-PDMS, while lower than 184-PDMS, exceeds that of h-PDMS and s-PDMS; the physical toughness of hù-PDMS, 184-PDMS, h-PDMS, and s-PDMS are 0.41, 4.77, 0.02, and 0.13 MPa, respectively.

hù-PDMS stamp provides a relatively high tensile modulus as compared to those of 184-PDMS and s-PDMS and an elongation at break that is much higher than that of h-PDMS; the tensile moduli of hù-PDMS, 184-PDMS, h-PDMS, and s-PDMS are 3.4, 1.8, 8.2, and 0.6 MPa, respectively.

These properties make hù-PDMS stamp easier to handle than the brittle material of h-PDMS and less susceptible to mechanical instabilities (e.g., mechanical collapse of tall, narrow lines) than 184-PDMS.

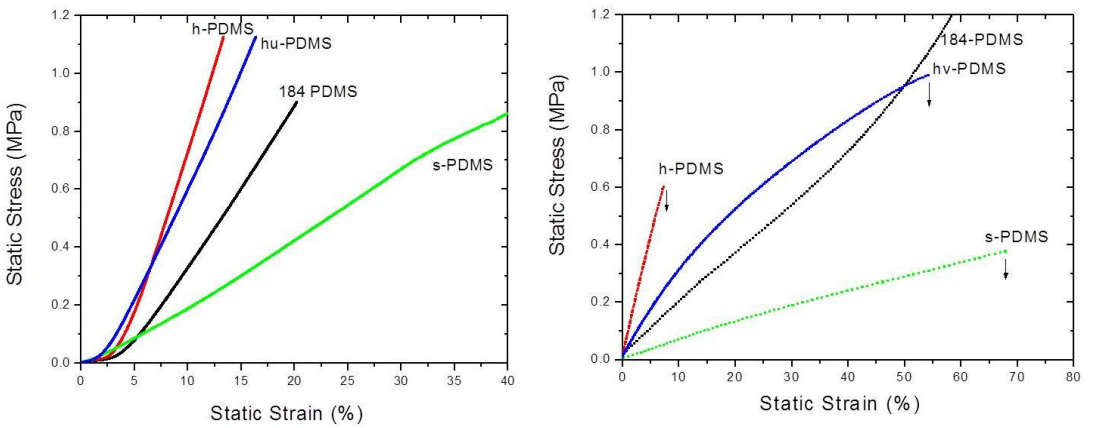

FIGURE 3.5
(left) Static compressive stress/strain curves and (right) static tensile stress/strain curves for four PDMS stamps, which were used to calculate their static tensile moduli from the slopes of Figure 3.5 (left). [14, 15]

Enhanced performance [15]

The improved mechanical strength of hù-PDMS stamp has direct benefits for soft lithographic performances.

Furthermore, the hù-PDMS stamp also has a photocurable capability, which is free from thermal shrinkages. The hù-PDMS prepolymer contains a cross-linker based on an urethane(methacrylate) pendant group, which is photocurable.

Low shrinkage is important, especially for high fidelity/resolution soft lithography that requires multilevel pattern registration over a large area. Shrinkage upon a polymerization was measured for each material using stamps formed by casting and curing the corresponding prepolymers against patterns of photoresist on silicon wafer substrates.

For linear shrinkage measurements, an original master and a PDMS mold were placed under a microscope. An image in the original master was chosen to calculate shrinkage. An exact length of the chosen image on both the master and the PDMS mold was measured by the microscopy. Shrinkage upon polymerization was calculated from a difference in length of the corresponding images between on the original master and the PDMS mold.

Comparing the lateral dimensions of the relief features on these PDMS molds to those on the "masters" reveals the dimensional changes due to curing. The hù-PDMS system has a linear polymerization shrinkage that is much lower than the commercial photocured s-PDMS, somewhat lower than h-PDMS, and slightly lower or comparable to the 184-PDMS; the polymerization shrinkages of hù-PDMS, 184-PDMS, h-PDMS, and s-PDMS are 0.6, 1.1, 1.6, and 3.1 %, respectively.

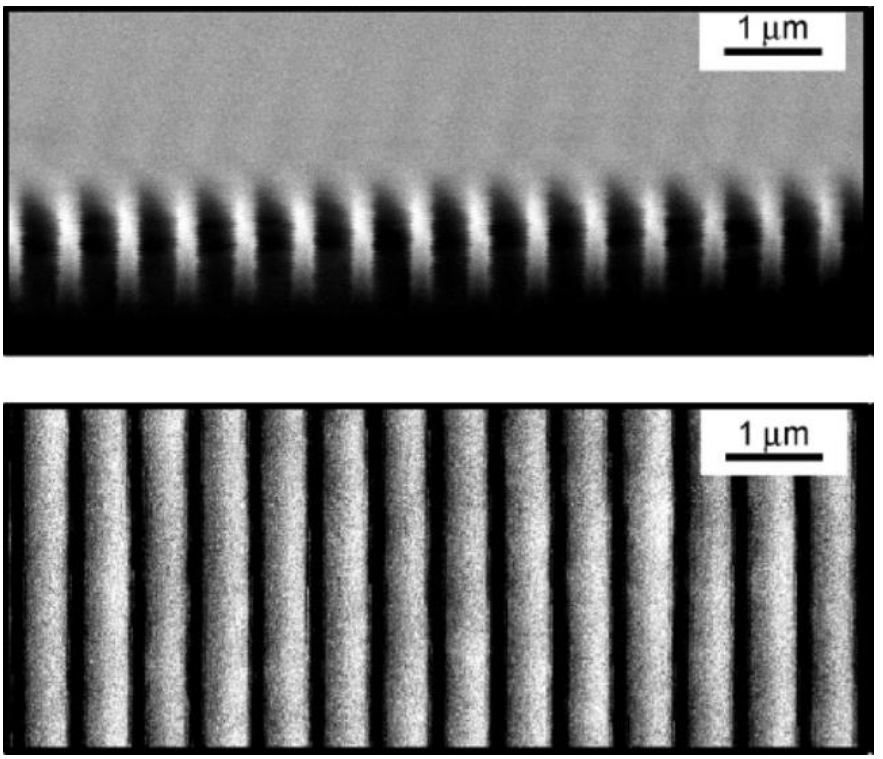

FIGURE 3.6
SEM images of the original master (top) and the surface relief feature on the hù-PDMS stamp (bottom) [15]

To establish the lithographic performance of hù-PDMS, we demonstrated the use of hù-PDMS for a patterning task that is not well suited to the other commercial PDMS elements: stamping with an elastic mold formed by curing against masters that have high aspect ratio, submicron features.

For the case described, an original master consists of 600 nm of thicknesses and 300 nm of wide lines of photoresist, with 300 nm spaces was prepared for the evaluation of the lithographic performance by using the hù-PDMS stamp. The top image in Figure 3.6 shows a SEM image of a cross-section view of the original master revealing the 600 nm of thicknesses and 300 nm of wide lines of the photoresist.

The bottom one in Figure 3.6 also shows a SEM image of the surface relief feature on the hù-PDMS stamp; as shown in the SEM image, the surface relief features replicated onto the hù-PDMS mold accurately corresponds to the features on the original master on the top image.

Subsequently, we also carried out “stamping process” by using different PDMS stamps for a comparison using the original master shown in Figure 3.6 (top image). Both of the 184 PDMS and the hù-PDMS molds were prepared using the original master (Figure 3.6, the top image) and then transferred patterns onto an optical adhesive layer (NOA 72, Norland).

Figure 3.7 shows SEM images of patterns generated on the optical adhesive layer using both of the 184 PDMS and the hù-PDMS molds for a comparison. The patterns transferred to the optical adhesive layer reveal an exceptionally comparative lithographic performance.

Our attempt to make a stamp out of 184-PDMS prepolymer using the original master failed; the result is shown in Figure 3.7 (left); the lithographic performance using 184 PDMS stamp results in the nano-lines disconnected, merged or tangled. It was because of mechanical feature collapse (Figure 3.7; left); adjacent lines in the 184-PDMS stamp tended to merge together in an uncontrolled fashion.

It is likely that the relatively low modulus of the 184-PDMS leads to this failure mode. In contrast, the same master was used to fabricate patterns using the hù-PDMS prepolymer; the result is shown in Figure 3.7 (right). It reveals a high fidelity in nanoresolution lithographic performance with the uniform and defect-free patterns over an area.

This excellent result has been one of the most challenging tasks to achieve in this area. Noteworthy results are the smooth edges, especially in the SEM image at highest magnification.

Furthermore, several hù-PDMS molds can be continuously generated from a single master without any damage; each stamp could be used multiple times for printing and molding processes.

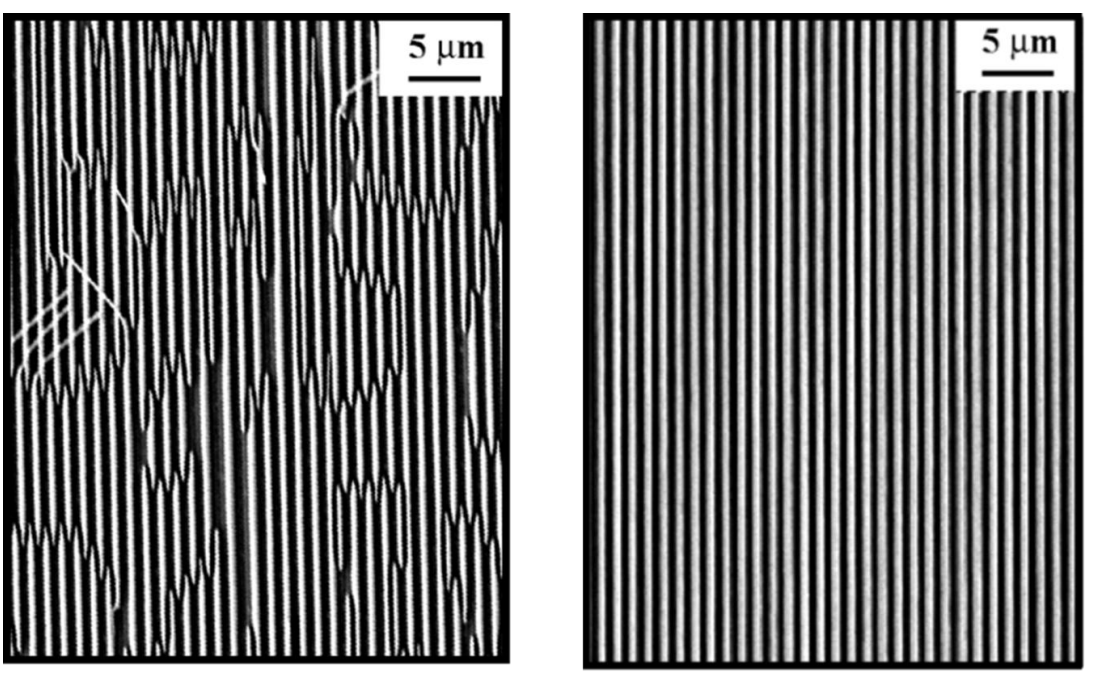

FIGURE 3.7
A comparison of soft lithography using the 184 PDMS (left) and the hù-PDMS (right) stamps [15]

As demonstrated in Figure 3.7, the resolution of fabricated patterns to the stamps' mechanical properties can significantly affect lithographic performance, particularly sharp reentrant features of relief near the contact surface of the stamp.

The controlled physical toughness of the hù-PDMS stamp also produced the high resolution at a large area, as shown in Figure 3.8 with different magnifications.

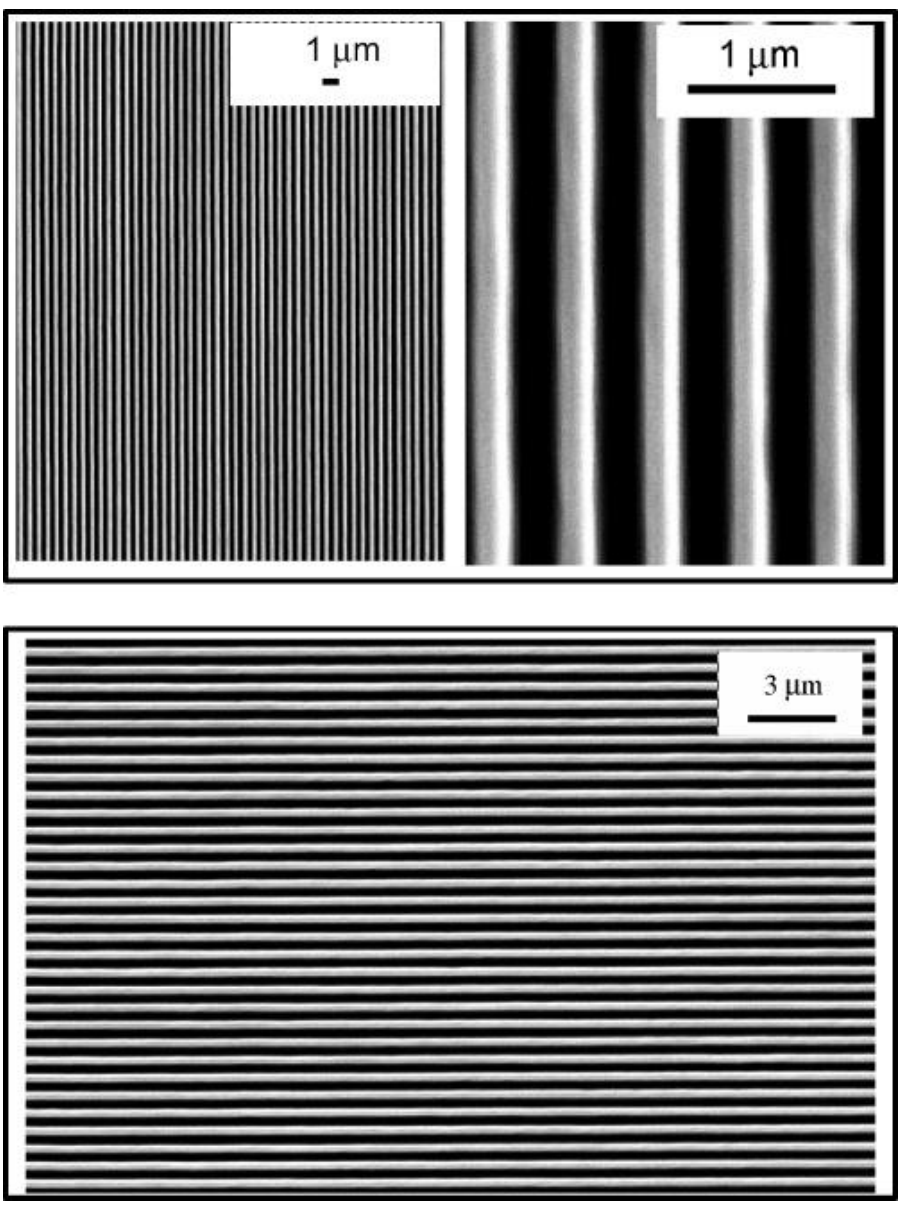

FIGURE 3.8
SEM images generated on the NOA optical adhesive using the hù-PDMS mold with a variety of magnifications [15]

Elastic Photopatterns

Benefits of the hù-PDMS system also include its photopatternable capability.

Elastic patterns are beneficial, for example, to fabricate compressive devices. However, elastomeric patterns fabricated using commercial silicon elastomers often results in mechanical failures and collapses with a poor fidelity that the edges disconnected, merged or tangled in an uncontrolled fashion. This task has been one of the most challenging projects to achieve in this area.

We use hù-PDMS prepolymer, a photopatternable elastomer, to fabricate elastic photopatterns. To generate elastic photopatterns on a chip, we prepared a quartz master with fine features (5-µm-width fine striped patterns) that filled in a square patterns. A 3-in. silicon wafer was used to fabricate the striped patterns on a chip using hù-PDMS prepolymer.

In our experiments, hù-PDMS prepolymer was spin-coated on the 3-in. of a silicon wafer. Subsequently, the quartz master was placed onto the hù-PDMS prepolymer layer as a photomask. The system was then exposed to a UV source (UVP Blak-Ray, B 100AP; 365 nm long wavelength UV) for 15-60 s, followed by soaking the system in an ethanol bath for 30 mins for a development.

The result is shown in Figure 3.9. The left microscopic image in Figure 3.9 shows elastic photopatterns fabricated over an area of a quarter section of the 3-in.-sized silicon wafer. The right image in Figure 3.9 also shows this same feature in higher magnifications.

Figure 3.9 reveals well-defined fine lines of 5 µm line width that fill in the square patterns. As seen in the magnified image at the right bottom, the resolution of photopatterns was calculated to be 5 µm.

In short, the hù-PDMS prepolymer has shown a promising photopatterning performance compared to those commercial PDMS systems; because, our chemical strategy creates new desired properties, which haven't been possible from the existing PDMS materials.

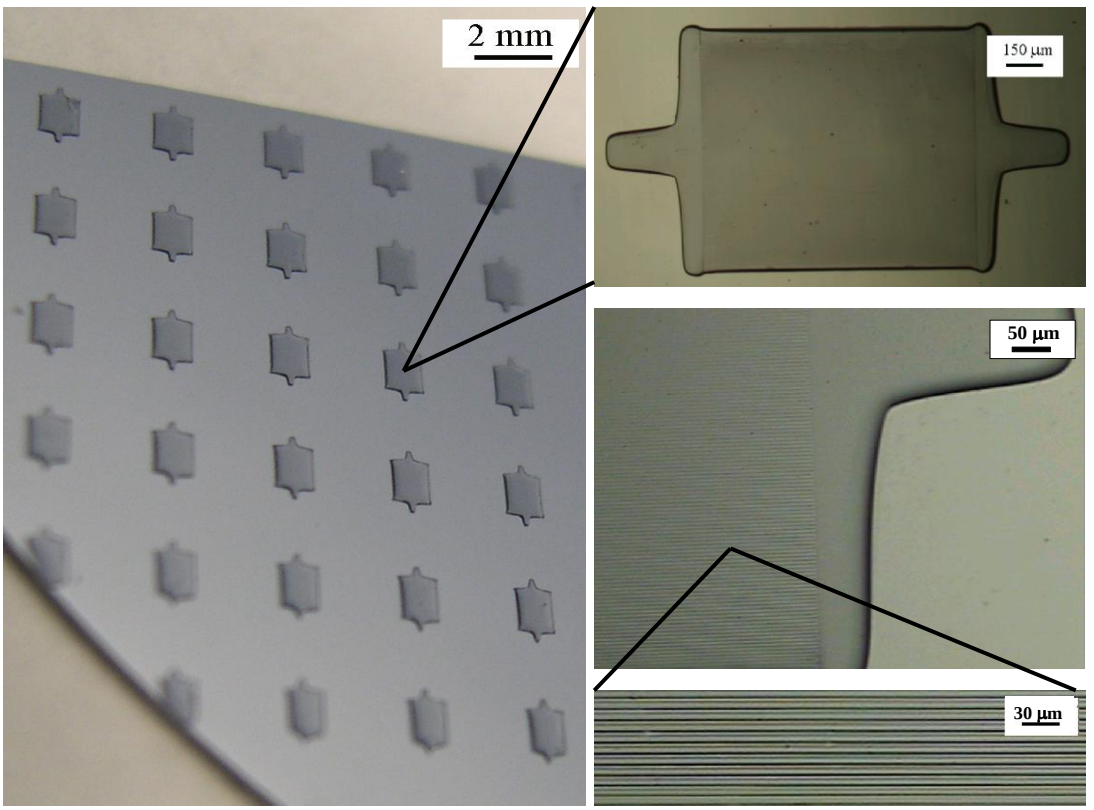

FIGURE 3.9
Elastomeric photopatterns generated on a silicon wafer using the hù-PDMS prepolymer [15]

Microfabrications

MIP's system has shown a limitation for practical applications, including the development of sensors at the micro- or nano-scale fabricated by controlled, fashionable integrations. To overcome the limitation, we demonstrate an identical integration by preparing a fluorescent template.

For an identical replica, we molecularly designed a fluorescent template; 9-ethyl adenine (compound # 1 in Figure 3.10) was chemically modified to synthesize a fluorescent template, an anthracene derivative (compound # 2 in Figure 3.10).

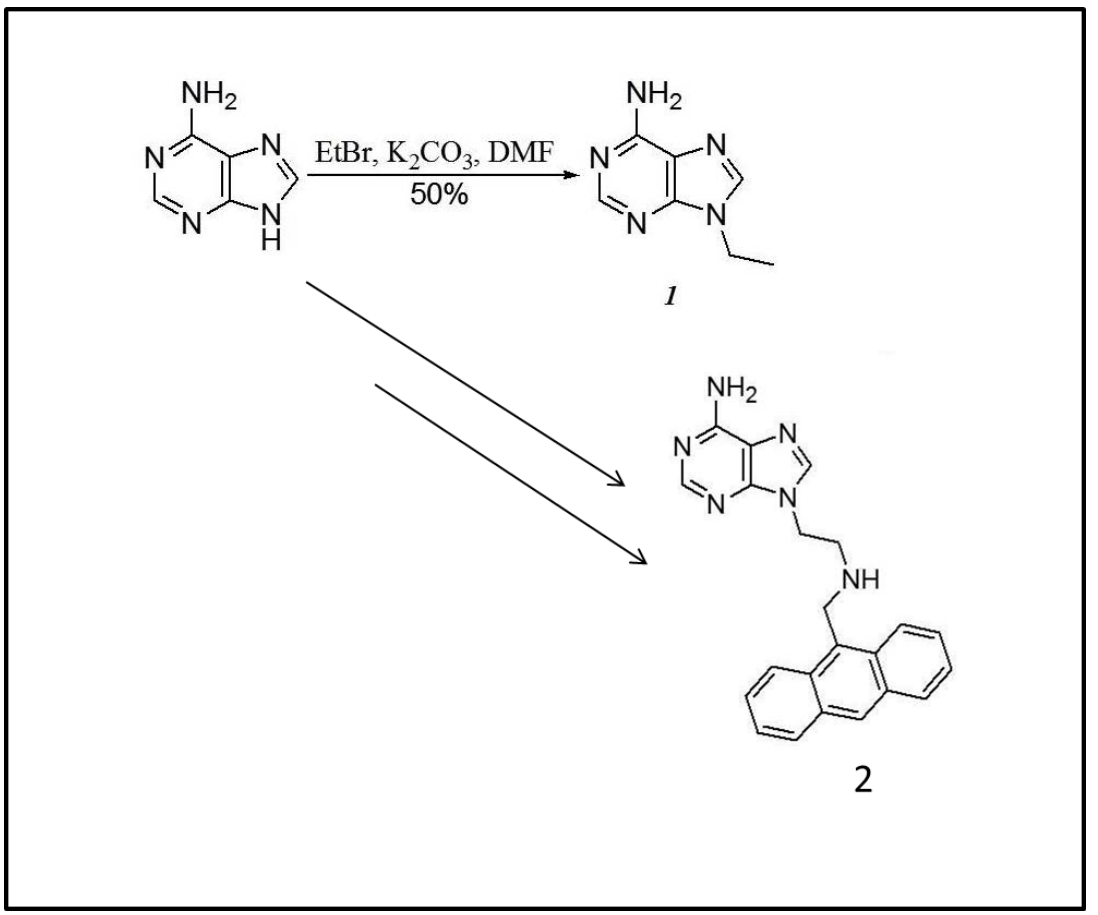

FIGURE 3.10
Syntheses of (top) 9-ethyl adenine and (bottom) 9-ethyl adenine anthracene derivative

For fluorescent microfabrications, an original master with a 2 µm of stripes and ~ 1 µm height was prepared by a photolithography. Using the original master, a 184-PDMS stamp comprised of the parallel linear channels with 2 µm wide was prepared by soft lithography.

For a patterning process, a glass substrate was cleaned and then coated with trichlorosilyl propylmethacrylate to attach the photocurable functionality on the glass surface.

A MIP's monomer mixture containing the fluorescent template was also prepared; it contains a functional monomer, methacrylic acid (MAA) (0.41g, 4.77mmol), ethylene glycol dimethacrylate (EGDMA) (cross-linker, 6.78 g, 34.21 mmol), and dimethoxy-2-phenyl acetophenone (0.103 g, 0.4 mmol) in toluene or acetonitrile or $CHCl_3$ (9.3 mL). The mixture was deoxygenated by a nitrogen for 5 mins. A template (approximately 0.4 mmol) was then added into the mixture then it was further deoxygenated.

The MIP's mixture was then dropped on the glass slide. Subsequently, the 184-PDMS stamp was placed on the top of the MIP's layer; the 184-PDMS stamp was used as a photomask for a

photocuring process. MIP's pattern was fabricated through a microcapillary molding technique (MIMIC). [44] It was photocured through the PDMS photomask by a UV radiation at 365 nm for 5 mins, followed by rinsing with MeOH for a development process. The PDMS stamp was then carefully removed to reveal the MIP patterns.

For a comparison, a control solution was also prepared by excluding the template. Both of the control and the MIP's solutions were prepared to fabricate photocured MIPs' patterns by MIMIC technique [44] under a same experimental condition. The control solution didn't contain the florescent template. Figure 3.11 shows fluorescence microscopic images of MIPs' patterns fabricated with and without the fluorescent template. It shows a comparative patterning performance between optically non-functional and functional patterns based on the fluorescent template.

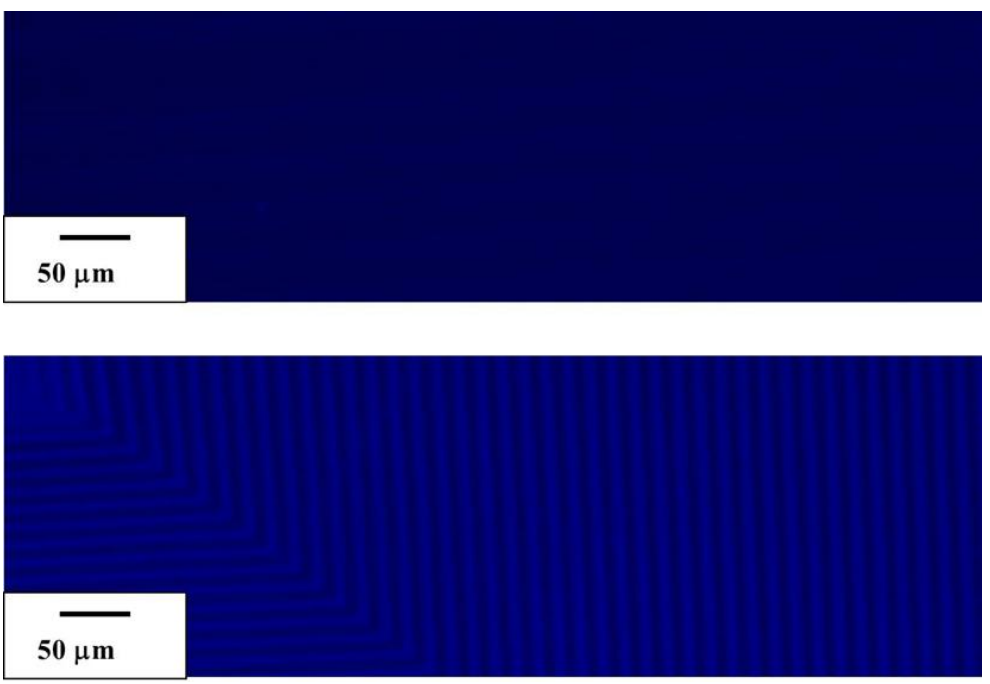

FIGURE 3.11
Fluorescence microscope images of MIPs' Patterns without (top) vs with (bottom) the fluorescence template

Figure 3.11 (top) shows a pattern fabricated by using a control solution without the fluorescent template. After the rebinding of the fluorescent template, it reveals the fluorescent image shown in Figure 3.11 (bottom). As shown in comparative fluorescent images in Figure 3.11, MIP's system can be fabricated as fashionable and controlled patterns on a glass. This is a promising result of integrating MIP's photopatterns fabricated on a glass substrate at the micro-scale.

Figure 3.12 also demonstrates comparative fluorescent microscopic images of MIP's patterns with and without the fluorescent template. The images clearly reveal those line patterns with 2 μm of width.

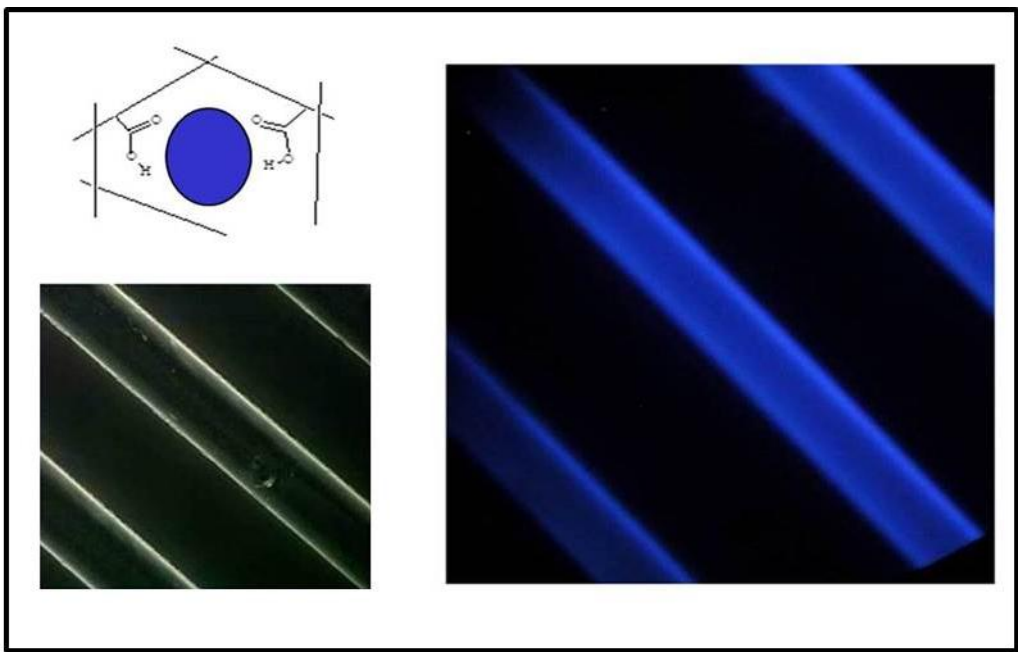

FIGURE 3.12
Fluorescence microscopic images of MIP's patterns with (left) and without (right) the fluorescent template. All of lines have a line-width of 2 μm

Microfluidic Synthesis [26]

Microfluidic synthesis has been widely used for the synthesis of novel materials/particles at the nano- or micro-scale; because, materials/particles prepared by the microfluidic synthesis have shown specific advantages, which couldn't be achieved by conventional bulk-scale synthesis. [20-30]

Especially, high chemical homogeneity can be achieved by mixing multiple components in microreactors, which are specifically designed for our diverse applications. Microfluidic reactors can be coupled to additional processing steps and directly integrated on a chip.

MIP's based sensors limit for a practical application due to its low sensitivity. Since detection is elicited by changing the physicochemical property of the interfaces, the development of high affinity recognition sites is crucial.

As mentioned in High Affinity Distribution Section, the particle sizes of MIP's system are directly related to their affinity capability of specific molecular recognition. [42] This motivates us to produce smaller sized MIP's particles to increase the sensitivity of sensors. We devoted our efforts to evaluate a practical application for the synthesis of robust 'monoclonal' MIP's particles to achieve a high affinity. In other words, MIP's particles at the nano- or micro-scale would contain

relatively smaller number of binding sites and is of a mass, which gives us the better chance for high affinity sites.

Due to our stringent needs for advanced sensors, we employed a microfluidic technique to synthesize smaller MIP's particles. Usually, microfluidic synthesis results in significant improvements, especially in mixing efficiency and better in control concentrations of reagents compared to conventional synthesis. [20-30]

Further selectivity based upon their affinity by gradient elution from the affinity zone permitting isolation of the highest fidelity particles was also considered.

Soft lithography enables to fabricate a number of novel microfluidic reactors; we designed a novel microfluidic channel pattern for the synthesis of MIPs' particles at the nano- or micro-size. A free standing PDMS stamp with a designed microchannel was prepared by soft lithography. Figure 3.13 shows a free standing PDMS stamp with the channel pattern to generate monodispersed picoliter to femtoliter sized MIPs' droplet emulsions at controlled rates.

As shown in Figure 3.13, the microfluidic channel consists of two inlets (30 µm channel width) and two outlets (the inner switchback with 30 µm width and the outer channel with 200 µm width). It also shows the T-junction, where the immiscible reagent and carrier fluid were fused. These variables were adjusted to optimize performance of the microfluidic reactor, which results in highly controllable droplet formations; because dynamic droplet generation also depends upon the absolute flow rate between the two phases.

A key parameter in the design of microchannels is to have the droplet size to be nominally the size of the orifice neck opening so that the shear force gradient can be applied across the entire droplet. These droplets generated at the T-junction will then be separated out. The reagent fluid will be the discrete phase inlet and the carrier fluid, which is an immiscible phase, will be the continuous phase inlet.

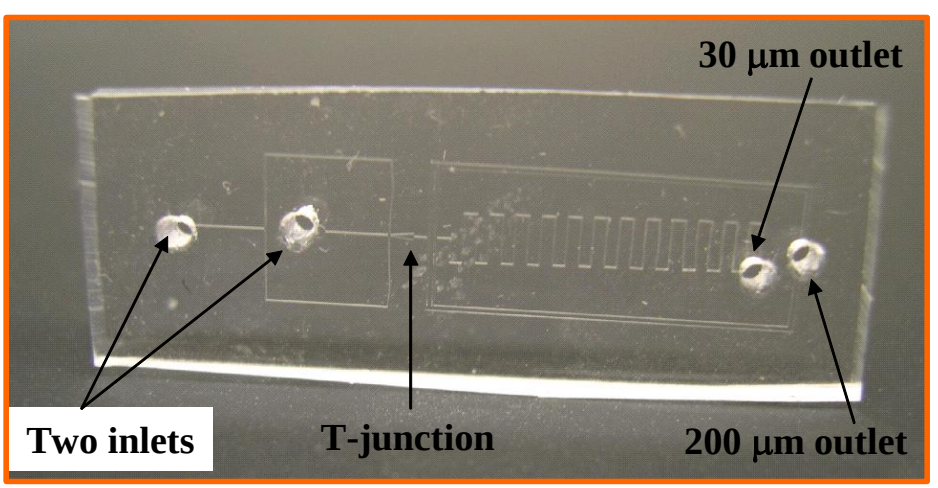

FIGURE 3.13
Microchannel pattern fabricated on a free standing PDMS stamp [26]

To produce MIP's droplets in the designed microfluidic reactor, a mixture of MIPs' monomer in toluene was prepared as a reagent flow. The MIP's monomer mixture contains methacrylic acid (MAA, 0.21 g, 2.40 mmol), ethylene glycol dimethacrylate (EGDMA, 3.41 g, 17.2 mmol), 9-ethyl adenenine (template; 0.02 g, 0.12 mmol, compound # 1 in Figure 3.10), and 2-2¬dimethoxy-2-phenyl-acetophenone (photo initiator; 0.033 g, 0.20 mmol) in toluene (4.5 mL). Water was used as a carrier fluid to generate MIPs' droplets at the T-junction.

Microfluidic platform was controllably generated monodispersed MIPs' droplets without using any surfactant; because, water was used as a carrier fluid. Syringe pumps were used to inject and then control the flow rates of reagents and carrier fluid.

MIP's droplets were generated at the opened T-junction, where the two immiscible phases merged by controlling flow rates; pumping rates of the reagent and the water fluids were 1.0-1.5 µL/min and 2.5µL/min, respectively.

The MIPs' droplet formation takes place as the individual nano- (satellite) or micro- (primary) sized MIPs' droplets at the T-junction and then these droplets were travelling along the outer microfluidic channel.

Subsequently, droplets were photocured through the PDMS photomask using an UV light at 365 nm. (Omnicure, cat #: 1000, power 20 W/cm^2 at a wavelength ~365 nm) Figure 3.14 shows MIPs' particles (a) primary droplets and (b) satellite droplets in dynamic motions before photopolymerization. Figure 3.14 (c) also shows MIP's particles after a photocuring process.

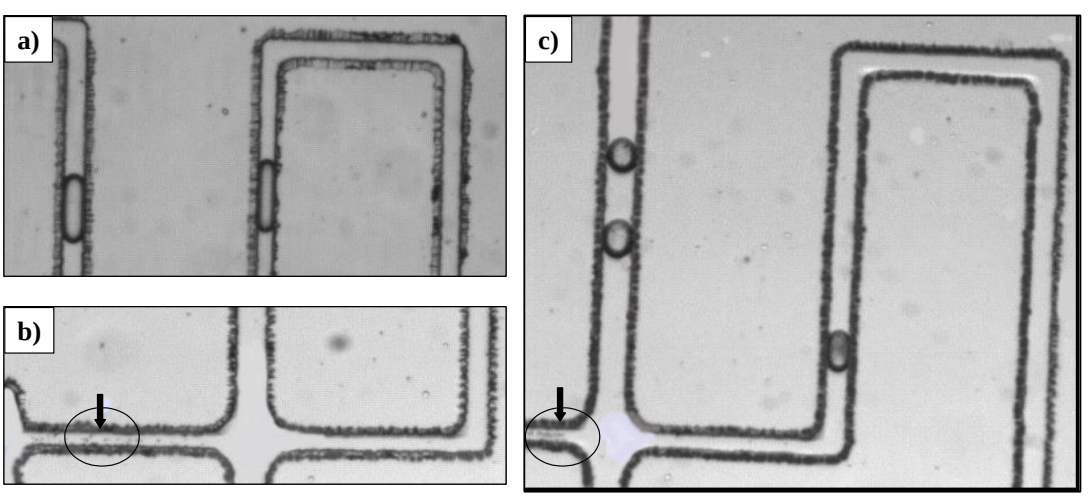

FIGURE 3.14
MIPs' droplets before (a and b) and after (c) photopolymerization; the channel width is 30 µm. Micro-sized primary droplets in 30 µm and nano-sized satellite droplets are observed [26]

Figure 3.14 also reveals a difference between before and after photopolymerizations; the dynamic flow motion shown in Figure 3.14 (a and b) before photopolymerization was dramatically changed in Figure 3.14 (c) after polymerization.

It also reveals a change in their refractive indices before (Figure 3.14 a and b) and after (Figure 3.14 c) photopolymerization; MIPs' droplets in Figure 3.14 (c) shows optically cloudy droplets while those in Figure 3.14 (a and b) shows optically clear droplets.

To establish the photopolymerization, we also carried out a FT-IR characterization of photocured MIPs' droplets shown in Figure 3.14 (c).

After the photopolymerization, a FT-IR spectrum was obtained. (Figure 3.15) As shown in the IR result, identical peaks of double bonds at 1640 and 888.3 cm^{-1} disappeared after the photocuring process. Additionally, the C-H stretching (out of plan) in methacrylate at 1715 cm^{-1} peak was blue-shifted to 1735 cm^{-1} after the photocuring step, which indicates a completion of polymerization. (Figure 3.15)

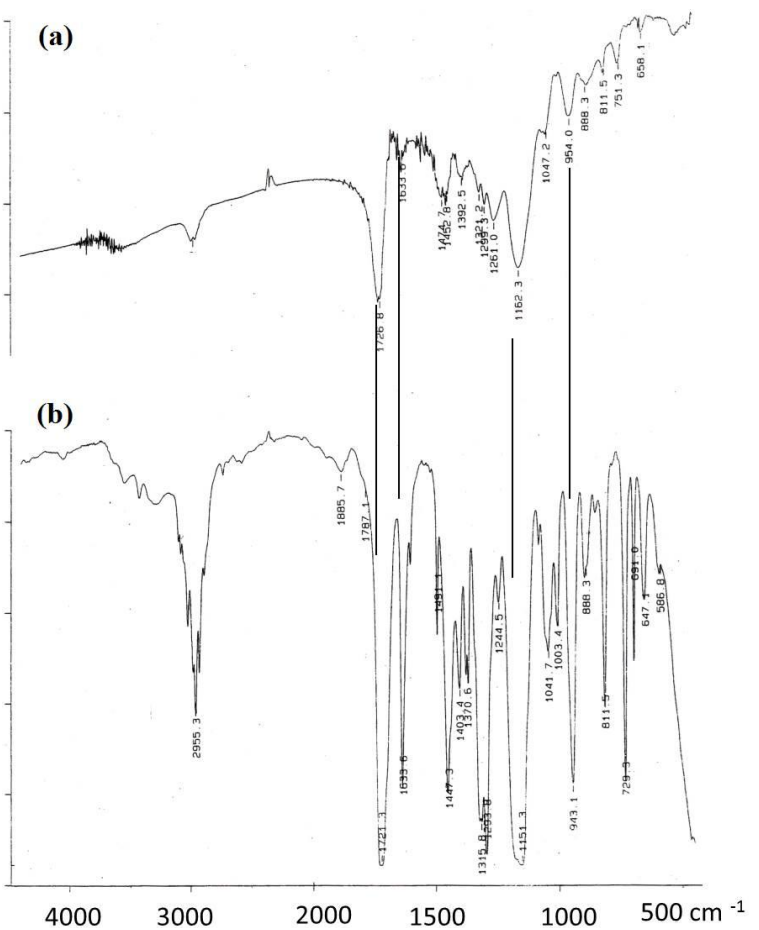

FIGURE 3.15
FT-IR spectra of photocured MIPs' particles (a) after and (b) before the photopolymerization; identical peaks of double bonds at 1640 and 888.3 cm^{-1} disappeared after the photocuring. Additionally, the C-H stretching (out of plan) in methacrylate at 1715 cm^{-1} peak was blue-shifted to 1735 cm^{-1} after the photocuring process which indicates a polymerization [26]

The ultimate goal of the microfluidic synthesis of MIP's particles is to prepare 'monoclonal' MIP's particles in the nano- or micro-size that contain high affinity binding sites only to increase the sensitivity and selectivity of sensors.

Conclusions

There are growing interests for state-of-the art sensors, such as wearable or disposable devices. More compact sensors/detection devices for a variety of applications such as medical diagnosis, optoelectronic communications, bio-chemical analysis, homeland security, and military defenses are desperately required. To satisfy our demands in detection technology, recent developments in nanotechnology are demonstrated in this chapter; soft lithography, microfabrication, and microfluidic synthesis are represented to develop high performance sensors.

"Molecularly Imprinted Polymer (MIP)", is introduced here as a promising sensing material based on synthesized receptor or binding sites. Furthermore, chemical strategies are also demonstrated in this chapter to achieve high performances in sensor technology.

Soft lithography allows us to fabricate flexible electronics, including wearable or disposable sensors at a low cost. However, the resolution of soft lithography limits, especially at the nano-sized regime. Also, commercial stamps are thermally cured materials, which are limited to generate photopatternable patterns.

To overcome the limitations, we modified the molecular structure of PDMS prepolymers to create our desired properties; urethane methacrylate groups were inserted into the cross-linkers. The resulting PDMS stamps showed enhanced physical toughness, reduced shrinkage, and a photopatternable capability. Nano-scaled soft lithography was demonstrated using a master consists of 600 nm thicknesses and 300 nm of wide lines with 300 nm spaces.

In elastic photopatterns, a master with 5 μm features was prepared. Photocurable PDMS prepolymers were used to fabricate features on a chip using the master; elastic photopatterns in a resolution of 5 μm was generated on a chip. It was a promising result that can fabricate elastic photopatterns, for example, compressive devices.

MIP's system was also examined for microfabrications. To identify MIP's patterns at the micro-scale, we chemically designed a fluorescent template. A master with 2 μm line patterns was used to fabricate MIP's patterns with and without the fluorescent template. Comparative fluorescent images of MIP's patterns with and without the fluorescent template were demonstrated. This result is promising to generate MIP's patterns with fashionable integrations on a chip for sensor applications.

Microfluidic synthesis was also employed to prepare small MIP's particles; because, smaller MIP's particles would have more high affinity sites and thus produce better sensitivity and selectivity. By designing a novel microreactor with 30 μm of channel widths, both of nano and micro-sized MIP's particles were produced. The particles at the nano or micro-sizes are a good candidate to develop high performance sensors/detection devices at the nano- or micro-scale.

Acknowledgements

The author thanks to Professor Kenneth J. Shea at UC-Irvine and Professor John Rogers at UIUC for helpful supports on this project.

References

1. Bawendi M G, Steigerwald M L, and Brus L E. The Quantum Mechanics of Larger Semiconductor Clusters.
   Annual Review of Physical Chemistry 1990; 41, 477-496.
2. Murray C B, Norris D J, and Bawendi M G. Synthesis and Characterization of Nearly Monodisperse CdE (E = sulfur, selenium, tellurium) Semiconductor Nanocrystallites. J. Am. Chem. Soc. 1993; 115 (19) 8706–8715.
3. Sirringhaus H, Kawase T, Friend R H, Shimoda T, Inbasekaran M, Wu M, and Woo E P. High-Resolution Inkjet Printing of All-Polymer Transistor Circuits. Science 2000; 290 (5499) 2123-2126.
4. Rogers J A, Bao Z, Baldwin K, Dodabalapur A, Crone B, Raju V R, Kuck V, Katz H, Amundson K, Ewing J, and Drzaic P. Paper-like Electronic Displays: Large-area Rubber-stamped Plastic Sheets of Electronics and Microencapsulated Electrophoretic Inks. Proc. Natl. Acad. Sci. U.S.A. 2001; 98 (9) 4835-4840.
5. Duan X, Niu C, Sahi V, Chen J, Parce J W, Empedocles S, and Goldman J L. High-Performance Thin-Film Transistors using Semiconductor Nanowires and Nanoribbons. Nature 2003; 425 (6955) 274-278.
6. Keren K, Berman R S, Buchstab E, Sivan U, and Braun E. DNA-Templated Carbon Nanotube Field-Effect Transistor. Science 2003; 302 (5649) 1380-1382.
7. Sundar V, Zaumseil J, Podzorov V, Menard E, Willett R L, Someya T, Gershenson M E, Michael E, and Rogers J A. Elastomeric Transistor Stamps: Reversible Probing of Charge Transport in Organic Crystals. Science 2004; 303 (5664) 1644-1646.
8. Moeller S, Perloy C, Jackson W, Taussig C, and Forrest S R. A Polymer/Semiconductor Write-Once Read-Many-Times Memory. Nature 2003; 426, 166-169.
9. Kanea R S, Takayamaa S, Ostunia E, Ingberb D E, and Whitesides G M. Patterning Proteins and Cells using Soft Lithography. Biomaterials 1999; 20 (23–24) 2363–2376.
10. Xia Y, Rogers J A, Paul K E, and Whitesides G M. Unconventional Methods for Fabricating and Patterning Nanostructures. Chem. Rev. 1999; 99 (7) 1823-1848.
11. Schmid H and Michel B. Siloxane Polymers for High-Resolution, High-Accuracy Soft Lithography. Macromolecules 2000; 33 (8) 3042-3049.
12. Odom T W, Thalladi V R, Love J C, and Whitesides G M. Generation of 30−50 nm Structures Using Easily Fabricated, Composite PDMS Masks. J. Am. Chem. Soc. 2002; 124 (41) 12112-12113.
13. Odom T W, Love J C, Wolfe D B, Paul K E, and Whitesides G M. Improved Pattern Transfer in Soft Lithography Using Composite Stamps. Langmuir 2002; 18, 5314-5320.
14. Choi K M and Rogers J A. A Photocurable Poly(dimethylsiloxane) Chemistry Designed for Soft Lithographic Molding and Printing in the Nanometer Regime. J. Am. Chem. Soc. 2003; 125 (14) 4060-4061.

15. Choi K M. Advanced Soft Lithography at the Nano-scale Regime; New Photocurable Silicon Elastomers with Adjustable Physical Toughness. J. Phys. Chem. B. 2005; 109 (46) 21525-21531.
16. Qin D, Xia Y, and Whitesides G M. Soft Lithography for Micro- and Nanoscale Patterning. Nature Protocols 2010; 5 (3) 491- 502.
17. Xia Y, Kim E, and Whitesides G M. Microcontact Printing of Alkanethiols on Silver and Its Application in Microfabrication. J. Electrochem. Soc. 1996; 143 (3) 1070-1079.
18. Huschka R, Zuloaga J, Knight M W, Brown L V, Nordlander P, and Halas N J. Light-Induced Release of DNA from Gold Nanoparticles: Nanoshells and Nanorods. J. Am. Chem. Soc. 2011; 133, 12247-12255.
19. Kim D H, Ghaffari R, Lu N, and Robers J A. Flexible and Stretchable Electronics for Biointegrated Devices. Annu. Rev. Biomed. Eng. 2012; 14, 113-128.
20. Thorsen T, Maerkl S J, and Quake S R. Microfluidic Large-Scale Integration. Science 2002; 298 (5593) 580-584.
21. Chan E M, Mathies R A, and Alivisatos A P. Size-Controlled Growth of CdSe Nanocrystals in Microfluidic Reactors. Nano Lett. 2003; 3 (2) 199-201.
22. Wu T, Mei Y, Cabral J. T, Xu C, and Beers K L. A New Synthetic Method for Controlled Polymerization Using a Microfluidic System. J. Am. Chem. Soc., 2004; 126 (32) 9880–9881.
23. Seo M S, Nie Z, Xu S, Mok M, Lewis P C, Graham R, and Kumacheva E. Continuous Microfluidic Reactors for Polymer Particles. Langmuir 2005; 21 (25) 11614–11622.
24. Hung L H, Choi K M, Tseng W Y, Tan Y C, Shea K J, and Lee A P. The Generation of CdS Nanoparticles by Dynamic Droplet Fusion; a Comparison of CdS Nanoparticles Prepared by Direct and Microfluidic Mixing. Lab Chip. 2006; 6, 174-178.
25. Choi K M. Unconventional Approaches for Advanced Nanotechnology; Functional Patterning and Microfluidic Synthesis. Mater. Res. Soc. Symp. Proc. 2006; 901E, Rb 09-01.
26. Choi K M. Microfluidic Approach for the Synthesis of Micro- or Nano-sized Molecularly Imprinted Polymer Particles. Research Letters in Materials Science 2008, 2008, 458158-458160.
27. Haeberlea S and Zengerleab R. Microfluidic Platforms for Lab-on-a-chip Applications. Lab Chip. 2007; 7, 1094-1110.
28. Masaya Miyazaki and Hideaki Maeda. Polymer Synthesis within Microfluidic Reactor. Encyclopedia of Microfluidics and Nanofluidics 2008; p. 1703-1710.
29. Chastek T Q, Iida K, Amis E J, Fasolka M J, and Beers K L. A Microfluidic Platform for Integrated Synthesis and Dynamic Light Scattering Measurement of Block Copolymer Micelles. Lab Chip. 2008; 8(6) 950-957.
30. Bouqueya M, Serraa C, Bertona N, Pratb L, and Hadziioannoua G. Microfluidic Synthesis and Assembly of Reactive Polymer Beads to form New Structured Polymer Materials. Chem. Eng. J. 2008; 135(1) S93–S98.
31. Huang X J and Choi Y K. Chemical Sensors based on Nanostructured Materials. Sensors and Actuators B. 2007; 122 (2) 659–671.
32. Guo X. Biosensors: Single-Molecule Electrical Biosensors Based on Single-Walled Carbon Nanotubes. Adv. Mater. 2013; 25 (25) 3390.
33. Madou M. Fundamentals of Microfabrication. CRC Press, Boca Raton, FL; 1997.
34. Conrad P G, Nishimura P T, Aherne D, Schwartz B J, Wu D, Fang N, Zhang X, Roberts J, and Shea K J. Functional Molecularly Imprinted Polymer Microstructures Fabricated Using Microstereolithography. Adv. Mater. 2003; 15 (18) 1541-1544.

35. Shea K J, Spivak D A, Sellergren B. Polymer Complements to Nucleotide Bases. Selective Binding of Adenine Derivatives to Imprinted Polymers. J. Am. Chem. Soc. 1993; 115 (8) 3368-3369.
36. Mosbach K. Molecular Imprinting. Trends in Biochemical Sciences 1994; 19(1) 9-14.
37. Shea K J. Molecular Imprinting of Synthetic Network Polymers: the De Novo Synthesis of Macromolecular Binding and Catalytic Sites. Trends in Polymer Science 1994; 2(5) 166-173.
38. Wulff G. Molecular Imprinting in Cross-linked Materials with the Aid of Molecular Templates - a Way Towards Artificial Antibodies. Angew. Chem. Int. Ed. 1995; 34(17) 1812-1832.
39. Spivak D A, Gilmore M A, and Shea K J. Evaluation of Binding and Origins of Specificity of 9-Ethyladenine Imprinted Polymers. J. Am. Chem. Soc. 1997; 119(19) 4388-4393.
40. Spivak D A and Shea K J. Binding of Nucleotide Bases by Imprinted Polymers. Macromolecules 1998; 31(7) 2160-2165.
41. Yan M and Kapua A. Fabrication of Molecularly Imprinted Polymer Microstructures. Analytica Chimica Acta. 2001; 435 (1) 163-167.
42. Umpleby R J, Baxter S C, Chen Y, Shah R N, and Shimizu K D. Characterization of Molecularly Imprinted Polymers with the Langmuir-Freundlich Isotherm. Anal. Chem. 2001; 73(19) 4584-4591.
43. Batra D and Shea K J. Combinatorial Methods in Molecular Imprinting. Current Opinion in Chemical Biology 2003; 7(3) 434.
44. Shea K J, Lee A P, and Yan M. Microfabrication of Molecularly Imprinted Polymers. PMSE Preprints 2004; 90, 160-161.
45. Huang H C, Lin C I, Joseph A K, and Lee Y D. Photo-Lithographically Impregnated and Molecularly Imprinted Polymer Thin Film for Biosensor Applications. J. Chromatogr. A. 2004; 1027 (1-2) 263-268.
46. Rushton G T, Furmanski B, and Shimizu K D. Plastic Antibodies: Molecular Recognition with Imprinted Polymers. J. Chem. Eng. 2005; 82 (9) 1374-1377.